where

$$A \equiv \alpha_0\alpha_1/(\alpha_0-\alpha_1).$$

One can see by inspection that

$$B(-\nu)=B^*(\nu), \quad \textstyle\sum_j R_j(-\nu)=\sum_j R^*(\nu). \quad \text{(A.11)}$$

We therefore have

$$\int_{-\infty}^{\infty} d\nu\, Z(\nu)Z(-\nu)=\int_{-\infty}^{\infty} d\nu\,|Z(\nu)|^2. \quad \text{(A.12)}$$

It is easily seen that the main contribution to the integral (A.12) comes from the neighborhoods of $\nu=\pm\omega$, and the contributions from both neighborhoods are equal. Setting $x=\nu-\omega$ we have, in the neighborhood of $\nu=\omega$,

$$R_5 \approx \frac{x(2x-i\beta)e^{i(\omega+x)t}}{2(ix-\alpha_0)(ix-\alpha_1)}. \quad \text{(A.13)}$$

Also, in the same neighborhood, R_2 and R_4 are negligible compared with R_1 and R_3, and the second term in $B(\nu)$ is negligible compared to the first. We can thus write

$$Z(\nu)_{\nu\sim\omega} \approx \frac{e^{i\omega t}}{\omega}\left[\frac{A}{2x-i\beta}\left(\frac{e^{\alpha_0 t}}{ix-\alpha_0}-\frac{e^{\alpha_1 t}}{ix-\alpha_1}\right)-\frac{xe^{ixt}}{2(ix-\alpha_0)(ix-\alpha_1)}\right], \equiv \tilde{Z}(x), \quad \text{(A.14)}$$

and

$$\int_{-\infty}^{\infty} d\nu\, Z(\nu)Z(-\nu)=2\int_{-\infty}^{\infty} dx\,|\tilde{Z}(x)|^2. \quad \text{(A.15)}$$

Substituting into Eq. (64), we obtain Eq. (65), with $\tilde{Z}$ replaced by $-\tilde{Z}^*$.

PHYSICAL REVIEW VOLUME 123, NUMBER 5 SEPTEMBER 1, 1961

Space-Charge Limited Current Relation in High-Pressure Gas Diodes

R. FORMAN
Parma Research Laboratory, Union Carbide Corporation, Parma, Ohio
(Received April 17, 1961)

A theory for space-charge conditions in high-pressure diodes has been developed which shows that the current obeys a $V^{\frac{1}{2}}$ power relation rather than the usual assumed V^2 relation. In addition, the theory predicts that the current in high-pressure diodes, at a constant anode voltage, varies as $p^{-\frac{1}{2}}$. Experimental data, taken in diodes filled with the inert gases, argon, neon, and helium, are presented to illustrate the validity of the theory.

THE Child-Langmuir[1] expression for space-charge conditions in a vacuum diode, showing that the current varies as the three-halves power of the voltage, has been verified by experiments over a wide range of conditions and been found to be true for any electrode that permits the escape of electrons or ions in a vacuum.

Although it is generally assumed that space-charge conditions apply to high-pressure gas diodes, there have been no widespread attempts to verify a relationship of this nature. The usual theoretical expression[2] which is considered applicable shows that the diode current follows a voltage-squared dependence given by

$$J=9.95\times10^{-14}kV^2/x^3 \text{(amp/cm}^2\text{)} \quad (1)$$

in the planar case and by

$$J=0.56\times10^{-12}kV^2/r^2 \text{(amp/cm)} \quad (2)$$

in cylindrical geometry. J is the current expressed in the units shown, k the mobility in cm^2/v sec, and x and r are anode distances in centimeters.

[1] I. Langmuir and K. T. Compton, Revs. Modern Phys. **3**, 191 (1931).
[2] J. D. Cobine, *Gaseous Conductors* (Dover Publications, Inc., New York, 1958), p. 129.

When space charge limited current measurements in high-pressure (1–300 mm) rare-gas diodes are made, they yield results which are at variance with the V^2 dependence of Eqs. (1) and (2). Figure 1 shows the

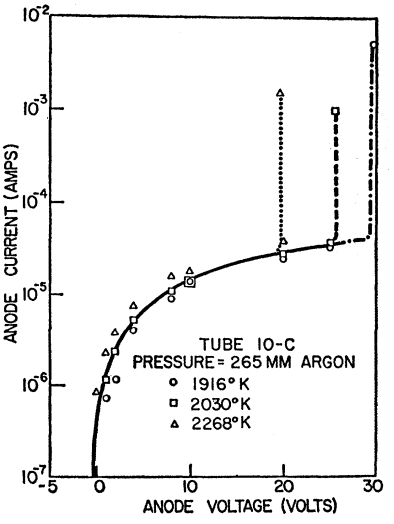

FIG. 1. Anode current-voltage characteristics of a cylindrical diode with a 0.009-in. diameter thoriated tungsten filament and a 1.0-cm diameter anode. The diode has an atmosphere of argon at 265 mm and the filament temperature is the other parameter.

results of some measurements in a cylindrical diode containing an ambient of argon at 265 mm mercury. If the data of Fig. 1 are analyzed, one finds they do not obey a J vs V^2 law. In addition, Eq. (2) yields results orders of magnitude too low to explain these data.

The concept of a constant electronic mobility is basic to the derivation of the above equations. However, the usual analysis of elastic scattering of electrons in a high-pressure gas does not lead to this result.[3,4] Instead, it indicates the following relation is valid.

$$v_d = c(E/p)^{\frac{1}{2}}, \tag{3}$$

where v_d is the drift velocity, c a proportionality constant, E the electric field, and p the pressure. An analysis of the space charge equation using the concept of the drift velocity proportional to $\sqrt{E}$ rather than proportional to E (constant mobility) yields a result more consistent with the experimental data.

If one assumes that the drift velocity in a high-pressure diode (where λ the mean free path for electrons is much smaller than the cathode-anode spacing) obeys Eq. (3), one obtains the following two relations:

$$d^2V/dx^2 = -4\pi\rho, \tag{4}$$

and

$$J = -\rho v_d = -\rho c[(dV/dx)/p]^{\frac{1}{2}}. \tag{5}$$

If Eq. (5) is solved for ρ, inserted into Eq. (4), which is then solved using the boundary conditions,

$$dV/dx = 0 \quad \text{at} \quad x = 0, \tag{6a}$$

$$V = 0 \quad \text{at} \quad x = 0, \tag{6b}$$

one obtains

$$J = [cp^{-\frac{1}{2}}/6\pi(\tfrac{2}{5})^{\frac{1}{2}}](V^{\frac{5}{2}}/x^{\frac{5}{2}}). \tag{7}$$

Similarly it can be shown (see Appendix) that the space-charge equation in practical units for a diode with cylindrical symmetry is

$$J = 5.56\times10^{-13} cp^{-\frac{1}{2}} \left\{ \frac{V_a}{F(r_a,r_c)} \right\}^{\frac{5}{2}} \text{amp/cm}, \tag{8}$$

where $F(r_a,r_c)$ is defined by Eqs. (A8) and (A9). A plot of $F(r_a,r_c)$ is shown in Fig. 2 showing its variation in units of r_a (anode radius) as a function of the ratio of anode to cathode radius. Figure 2 shows that when $r_a \gg r_c$, Eq. (8) approaches

$$J = 5.56\times10^{-13} \frac{cp^{-\frac{1}{2}}}{r_a^{\frac{5}{2}}} V_a^{\frac{5}{2}} \text{ amp/cm}. \tag{9}$$

Equations (7), (8), and (9) indicate two unique features of high-pressure diodes which can be experimentally verified; namely, (1) J follows a $V^{\frac{5}{2}}$ dependence at constant pressure and (2) J follows a $p^{-\frac{1}{2}}$ dependence at a constant anode voltage.

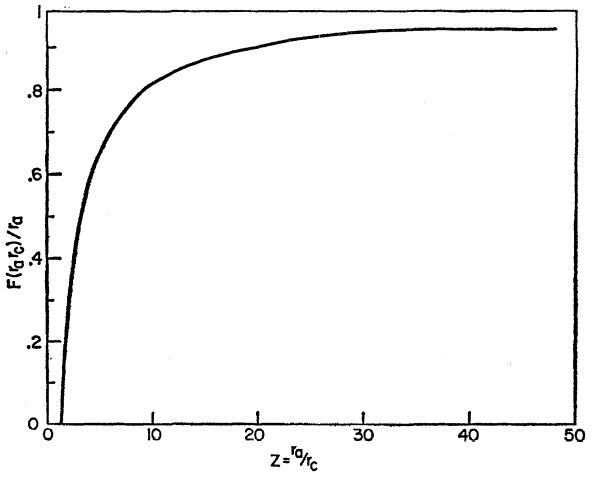

FIG. 2. $F(r_a,r_c)/r_a$ vs z, r_a is the anode radius, r_c is the filament radius, and z is the ratio of anode to filament radius.

[3] P. M. Morse, W. P. Allis, and E. S. Lamar, Phys. Rev. 48, 412 (1935).

[4] A. von Engel, *Ionized Gases* (Oxford University Press, New York, 1955), p. 104.

EXPERIMENTAL VERIFICATION

The two diode models used are illustrated in Fig. 3. These tubes were evacuated and processed on an ultra-high-vacuum system. The details of the vacuum and gas-handling system have been described elsewhere.[5]

The electronic circuits employed in these measurements are illustrated in Fig. 4. Figure 4(a) is the circuit

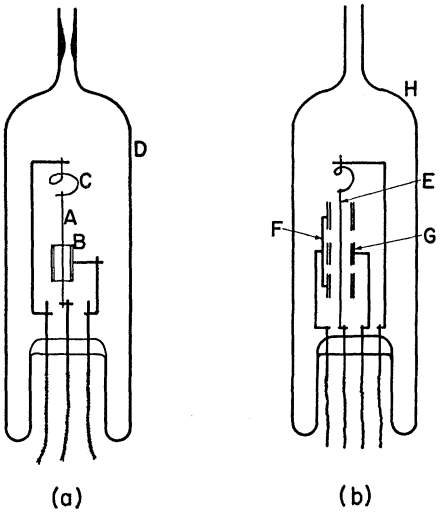

FIG. 3. (a) Cylindrical diode. A is the filament (about 0.01 in. diameter and 3.5 cm long). B is a tungsten or tantalum cylindrical anode 1 cm diameter and 1.25 cm long. C is a tantalum spring support and D a Pyrex glass envelope. The supporting leads were either tungsten or tantalum. (b) Guard-ring diode. E is a 0.01-in. diameter tungsten filament about 4 cm long. F is two guard-ring tantalum anodes approximately 1 cm in diameter, 1.28 cm length, and G is the center anode having the same diameter but being 0.64 cm long. H is a Pyrex envelope and the supporting leads were either tungsten or tantalum.

[5] R. Forman, J. Appl. Phys. 32, 1651 (1961).

used to test the ordinary cylindrical diodes and 4(b) is that used to test the guard-ring-type diodes.

Filament temperatures were determined by an application of the Jones-Langmuir[6] tables to the vacuum filament current. The temperature of the filament was then checked pyrometrically, through a small hole in the anode, by the use of a Pyro micropyrometer. After these measurements were made, the vacuum pyrometer settings for a given temperature were then used in succeeding experiments with high-pressure gases to set filament temperatures.

Figure 5 shows space-charge limited data plotted as J vs $V^{\frac{3}{2}}$ power for three high-pressure inert-gas diodes containing argon, neon, and helium. Although these data are all above 100 mm, it should be pointed out that similar experimental results were obtained with pressures down to 1 mm. They all showed the same linear relation between J and $V^{\frac{3}{2}}$ power.

Figure 6 is a plot of the current at a given anode voltage for tube 10C (used to obtain the data of Fig. 1) as a function of pressure to the minus one-half. Similar results are obtained in the neon and helium ambients.

These data verify the qualitative features of Eq. (8), which states that J vs $V^{\frac{3}{2}}$ and J vs $p^{-\frac{1}{2}}$ are linear. It was found, however, that the experimental slope of the J vs $V^{\frac{3}{2}}$ power curves were higher by at least a factor of 2 than the theoretical value given by Eq. (8). As an example, consider the helium data of Fig. 5. The slope of the J vs $V^{\frac{3}{2}}$ power plot is 2.6×10^{-7} amp/v$^{\frac{3}{2}}$. The theoretical value of the slope is dependent on the value of c given by Eq. (3), which can be obtained from the data of Pack and Phelps[7] or Brown.[8] From the latest data,[7] one can estimate that c for helium is approximately 1.0×10^{6} cm$^{\frac{3}{2}}$ (mm Hg)$^{\frac{1}{2}}$/v$^{\frac{1}{2}}$ sec to an accuracy of about 10–20%. If this value and the value of the geometrical dimensions of the tube [given by Fig. 3(a)] are inserted into Eq. (8), a theoretical slope of 1.1×10^{-7} is obtained which results in a value of 2.4 for the ratio of experimental to theoretical slope.

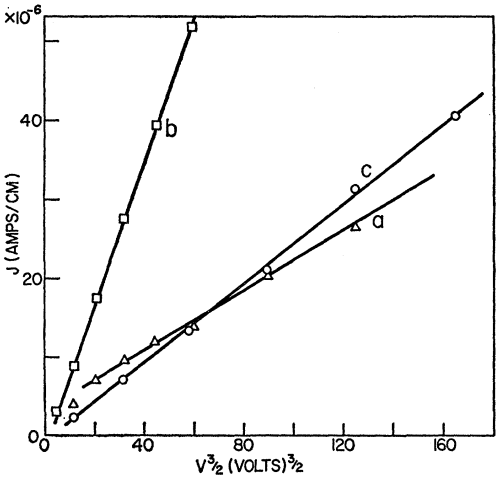

FIG. 5. Current vs (voltage)$^{\frac{3}{2}}$ for: (a) cylindrical diode 10C having a thoriated tungsten filament operating at 1916°K in an argon ambient at a pressure of 265 mm Hg; (b) cylindrical diode 7B having a tungsten filament operating at 2800°K in a neon ambient at a pressure of 123 mm Hg; (c) cylindrical diode 7B having a tungsten filament operating at 2800°K in a helium ambient at a pressure of 263 mm Hg.

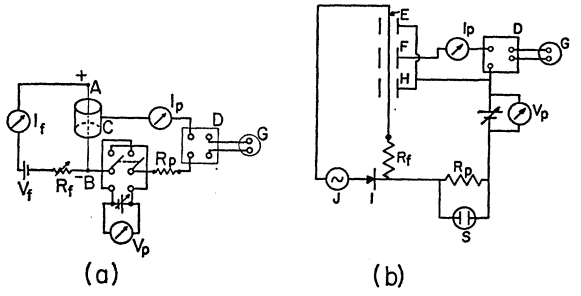

FIG. 4. (a) Electrical circuit for measuring current-voltage characteristic of the gas diodes shown in Fig. 3(a). AB is the filament and C the anode of the tube. The filament supply is V_f and the anode supply is measured by V_p. D is an Ayrton shunt and G a galvanometer. I_p is a milliammeter. (b) Electrical circuit for measuring current-voltage characteristic of the gas diode shown in Fig. 3(b). E is the filament, F the anode, H the guard-ring anode, and S is an oscilloscope. The filament circuit consists of a Variac source J, a half-wave silicon rectifier I, and a filament dropping resistor R_f. The top of the filament in this diagram was always positive during the forward half-cycle. The other electronic components in this diagram are the same as their counterparts described in (a).

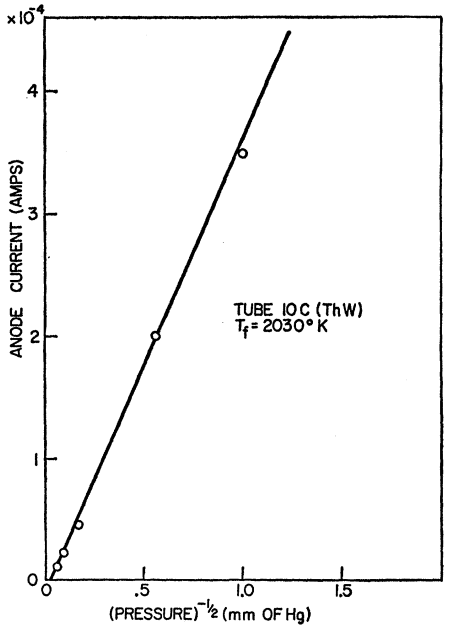

FIG. 6. Current vs (pressure)$^{-\frac{1}{2}}$ at a constant anode voltage of 8 v for cylindrical diode 10C having a thoriated tungsten filament operating at 2030°K. The ambient is argon and the pressure range was from 1 to 265 mm Hg.

[6] H. A. Jones and I. Langmuir, General Electric Rev. **30**, 310 (1927).

[7] J. L. Pack and A. V. Phelps, Phys. Rev. **121**, 798 (1961).

[8] S. C. Brown, *Basic Data on Plasma Physics* (The Technology Press of the Massachusetts Institute of Technology, Cambridge, Massachusetts, 1959).

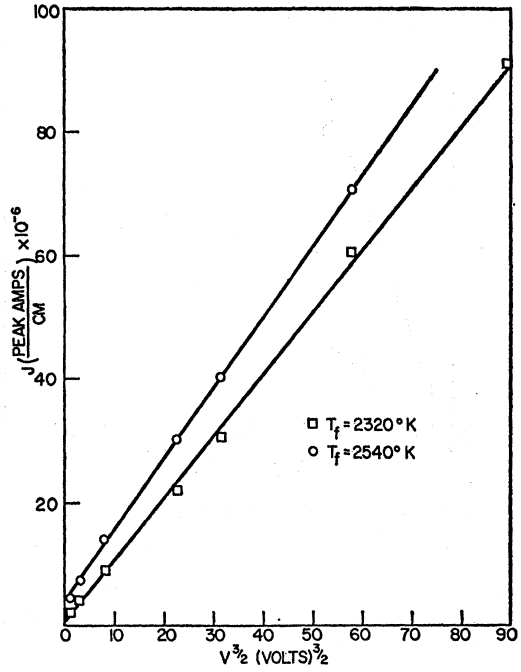

FIG. 7. Current vs (voltage)$^{\frac{3}{2}}$ for guard-ring diode 12B having a tungsten filament operating at temperatures of 2320° and 2560°K. The ambient is helium at a pressure of 37 mm Hg.

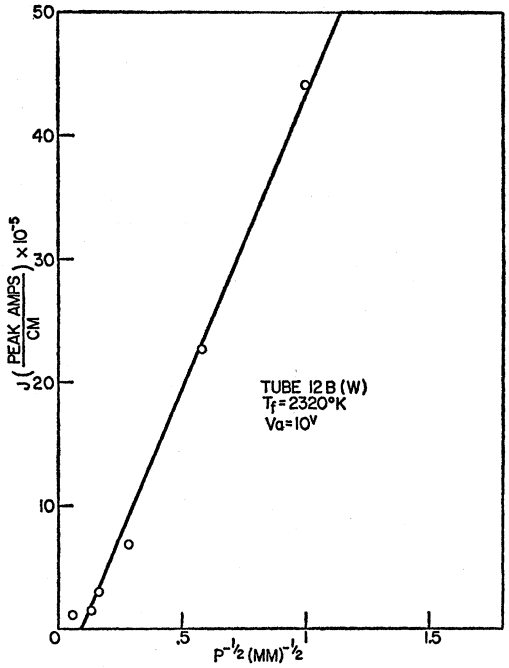

FIG. 8. Current vs (pressure)$^{-\frac{1}{2}}$ at a constant anode voltage of 10 v for guard-ring diode 12B having a tungsten filament operating at 2320°K. The ambient is helium and the pressure range was from 1 to 324 mm Hg.

There are two obvious difficulties involved in interpreting the previous data on ordinary cylindrical diodes. They are (1) the difficulty of eliminating edge effects on single anode structures and (2) the need for a dc filament voltage to heat the filament. To confirm the above results and to make more precise measurements of space-charge conditions, a tube identical to that in Fig. 3(b) was used in a circuit shown in 4(b). The use of the guard ring minimized any end effects and the circuit of Fig. 4(b) is a modification of that described by Harnwell and Livingood,[9] and is used to eliminate the effects due to a filament voltage drop. The voltage drop across R_f in the forward direction was about 90% of the total filament circuit voltage. The anode current pulse was a 60-cycle square wave. These measurements were made in a helium ambient and a typical result of J vs $V^{\frac{3}{2}}$ plot at 37 mm is shown in Fig. 7. These data were fitted by the method of least squares and a slope of 1.0×10^{-6} amp/v$^{\frac{3}{2}}$ for the 2320°K curve and 1.1×10^{-6} amp/v$^{\frac{3}{2}}$ for the 2540°K curve was obtained. If the theoretical value for the slope at this pressure is calculated from Eq. (8), one again finds that the experimental slope is greater than the theoretical slope; this time by a factor of 3.

Table I shows the comparison between theory and experiment for the guard-ring helium diode data as the pressure was varied from 1 to 324 mm. In addition, Fig. 8 is a plot of J vs $p^{-\frac{1}{2}}$ for these data taken in helium with the guard-ring type of diode.

A fairly simple explanation of these differences between theory and experiment and their variation with pressure exists. As the pressure decreases and the mean free path through the gas becomes comparable to tube dimensions, one can expect the slope of the J vs $V^{\frac{3}{2}}$ curve to become independent of pressure and approach 3.6×10^{-5} amp/v$^{\frac{3}{2}}$ (assuming r_a=0.415 cm), which is the vacuum characteristic slope.[1] An examination of Table I shows this to be true: At low pressures where the ratio difference is greatest one approaches the value of the vacuum slope. In addition, the theoretical values given in column 2 of Table I are derived by using the physical dimensions of the filament and anode (r_c=0.013 cm, r_a=0.415 cm) in obtaining the value of $F(r_a,r_c)$ from Fig. 2. In this case $F(r_a,r_c)/r_a$ is very close to unity. If the actual filament radius were taken as r_c=0.13 cm, the theoretical slope for the high-pressure data (37 mm or above) would be in excellent quantitative agreement with experiment. This assumption, that the virtual cathode has a larger radius than the geometrical cathode, is a valid one for the following reason. The basic assumption involved in the validity of Eq. (3), that v_d is proportional to $(E/p)^{\frac{1}{2}}$, is that the electron in the high-pressure gas attains its final drift velocity after it has gone through a distance orders of magnitude greater than the electronic mean free path. Since the electronic mean free path in helium at 100 mm

[9] G. P. Harnwell and J. J. Livingood, *Experimental Atomic Physics* (McGraw-Hill Book Company, Inc., New York, 1933), p. 210.

TABLE I. Comparison between theory and experiment for the guard ring helium diode data.

Helium pressure (mm Hg)	Theoretical slope of J vs $V^{\frac{3}{2}}$ (amp/v$^{\frac{3}{2}}$)	Experimental slope of J vs $V^{\frac{3}{2}}$ (amp/v$^{\frac{3}{2}}$)	Ratio of exp/theor slope
324	1.3×10^{-7}	3.2×10^{-7}	2.5
53	3.2×10^{-7}	7.3×10^{-7}	2.3
37	3.9×10^{-7}	1.0×10^{-6}	2.6
13	6.5×10^{-7}	2.0×10^{-6}	3.3
3	1.4×10^{-6}	7.1×10^{-6}	5.1
1	2.4×10^{-6}	1.3×10^{-5}	5.4

is approximately 5×10^{-4} cm, a virtual cathode at 1-mm radius would imply that the electrons undergo approximately 200 collisions before they attain the steady-state drift velocity given by Eq. (3). This seems to be a reasonable assumption.[4] No attempt was made to refine the theory by considering the thermal distribution of the emitted electrons because it is probable that the uncertainty in the position of the virtual cathode is the most significant error in the theory.

It should be mentioned that there seems to be experimental evidence that v_d follows a $(E/p)^{\frac{1}{2}}$ relation in argon at low field and high pressure.[7] If such a relation is substituted for Eq. (5) in a new derivation, the relation which follows predicts that J varies as $V_a^{5/4}$ and as $p^{-\frac{1}{4}}$. It may be possible to plot the argon data in Fig. 5 this way and obtain a reasonable straight line, but this is not true for the data in Fig. 6. A plot of these data as J vs $p^{-\frac{1}{4}}$ is not linear; however, J vs $p^{-\frac{1}{2}}$ is linear.

ACKNOWLEDGMENT

The author is indebted to J. R. Reiss for his assistance in the experimental program.

APPENDIX

In the case of cylindrical symmetry, the two equations needed to express space-charge conditions are

$$\frac{1}{r}\frac{d}{dr}\left(r\frac{dV}{dr}\right)=-4\pi\rho, \tag{A1}$$

$$J=-2\pi r\rho v_d=-2\pi r\rho c\left[(dV/dr)/p\right]^{\frac{1}{2}}. \tag{A2}$$

If ρ, evaluated from (A2) is substituted in (A1), one obtains

$$\frac{d}{dr}\left(r\frac{dV}{dr}\right)=K\left(\frac{dV}{dr}\right)^{-\frac{1}{2}}, \tag{A3}$$

where

$$K=2Jp^{\frac{1}{2}}/c. \tag{A4}$$

An integration of Eq. (A3) leads to the following solution:

$$\frac{dV}{dr}=\frac{1}{r}\left[A+Kr^{\frac{3}{2}}\right]^{\frac{2}{3}}, \tag{A5}$$

where A is an arbitrary constant of integration. If one now assumes the usual space-charge condition at the cathode, namely, the electric field is zero at the cathode radius r_c, the following equation results:

$$\frac{dV}{dr}=\frac{(K)^{\frac{2}{3}}}{r}\left[r^{\frac{3}{2}}-r_c^{\frac{3}{2}}\right]^{\frac{2}{3}}. \tag{A6}$$

If Eq. (A6) is solved using the boundary conditions $V=0$ at $r=r_c$, one obtains the solution

$$V=K^{\frac{2}{3}}F(r,r_c), \tag{A7}$$

where

$$F(r,r_c)=\frac{r}{z}\left\{(z^{\frac{3}{2}}-1)^{\frac{2}{3}}-\ln\frac{z^{\frac{1}{2}}}{1+(z^{\frac{3}{2}}-1)^{\frac{1}{2}}}-\frac{2}{\sqrt{3}}\tan^{-1}\left[\frac{2(z^{\frac{3}{2}}-1)^{\frac{1}{2}}-1}{\sqrt{3}}\right]-\frac{\pi}{3\sqrt{3}}\right\}, \tag{A8}$$

and

$$z=r/r_c. \tag{A9}$$

If the value of K from Eq. (A4) is inserted into (A7), the following relation results:

$$J=\tfrac{1}{2}cp^{-\frac{1}{2}}\{V/F(r,r_c)\}^{\frac{3}{2}}. \tag{A10}$$

Setting $V=V_a$ at $r=r_a$, the resulting space-charge equation in cylindrical geometry becomes

$$J=\tfrac{1}{2}cp^{-\frac{1}{2}}\{V_a/F(r_a,r_c)\}^{\frac{3}{2}}, \tag{A11}$$

relating the current per unit length of filament to the anode voltage. In practical units, Eq. (A11) becomes

$$J=5.56\times10^{-13}cp^{-\frac{1}{2}}\{V_a/F\}^{\frac{3}{2}}\ \text{amp/cm}, \tag{A12}$$

where $cp^{-\frac{1}{2}}$ is expressed in cm$^{\frac{3}{2}}$/v$^{\frac{1}{2}}$ sec, the anode and cathode radius in cm, and the anode voltage in volts.